RESEARCH PAPER

Receptor-Based Virtual Screening and Synthesis of Dual Inhibitors Targeting Alk and Ros1 Kinases in Lung Cancer

Dipali Kurkute[1], Rahul Lokhande[1]*, Kuldeep Ramteke[1], Kiran Shinde[2], Yogesh Gurav[3], Nilesh Bhosale[4]

[1]*Samarth Institute of Pharmacy, Belhe, Tal. Junnar, Dist. Pune, Affiliated to Dr. Babasaheb Ambedkar Technological University, Lonere, Dist. Raigad, Maharashtra, India*
[2]*Vidyaniketan Institute of Pharmacy and Research Center, Bota, Tal. Sangamner, Dist. Ahilyanagar, Affiliated to Dr. Babasaheb Ambedkar Technological University, Lonere, Dist. Raigad, Maharashtra, India*
[3]*Satara College of Pharmacy, Satara, Affiliated to Dr. Babasaheb Ambedkar Technological University, Lonere, Dist.-Raigad, Maharashtra, India*
[4]*PDEA's SGRS College of Pharmacy, Saswad, Pune, Affiliated to Savitribai Phule Pune University, Pune, Maharashtra, India.*

Received: 12th Aug, 2025; Revised: 11th Sep 2025; Accepted: 17th Nov, 2025; Available Online: 30th Nov, 2025

ABSTRACT
This paper reports on their design, synthesis, and testing of quinoline-3-carboxamides containing sulfonamide moieties, for potential ALK and ROS1 inhibitory activities for the treatment of non-small cell lung cancer (NSCLC). Lead compounds were identified through computational screening carried out using DrugRep Web Server based on the stability and the ability of these lead compounds to interact with receptor ATP-binding sites. Optimization of structure was necessary to enhance selectivity, lipophilicity, and ADMET properties by improving heterocyclic cores' configurations, substituents, and functional groups. It is established that 2-chloro-N-(4-hydroxyphenyl)quinoline-3-carboxamide has substantial potential as an inhibitor supported by pharamophore design. Therefore, the synthesis of ten derivatives was carried out with melting points established between 178 and 208 °C; while the Rf values lie within 0.48 and 0.60. They were purified to the high end with their response at the IR, ^{1}H NMR, and HRMS levels. Functional groups such as -OH, -Cl, and sulfonamide could now be incorporated for increased ALK and ROS1 kinase domain-binding. The synthesis of CQCS3 compound (90%) has shown that sulfonamide, too, has an occurrence in kinase binding with the highest yield and ALK-ROS1 kinase binding potential. These observations indicate quinoline-based derivatives might exhibit pertinent interest in precision oncology interventions for NSCLC treatments.
Keywords: Quinoline derivatives, ALK inhibitors, ROS1 inhibitors, NSCLC, Sulfonamide, Kinase inhibitors, Drug design, Virtual screening, Computational pharmacology, Precision oncology.
How to cite this article: Kurkute D, Lokhande R, Ramteke K, Shinde K, Gurav Y, Bhosale N, Receptor-Based Virtual Screening and Synthesis of Dual Inhibitors Targeting Alk and Ros1 Kinases in Lung Cancer. Int J Drug Deliv Technol. 2025;15(4):1666-1676, DOI: 10.25258/ijddt.15.4.18
Source of support: Nil.
Conflict of interest: None

INTRODUCTION

Lung cancer tops the list as a killer of cancer related deaths, holding a count of about 18% of all cancer deaths[1]. Out of the whole range of histological subtypes, NSCLC accounts for nearly 85%, and hence is the most common form[2]. The prognosis of NSCLC remains unfavorable despite great advances in diagnostic and therapeutic avenues, with the local or metastatic stages being more depressing indeed[3]. The chances of global survival over five years are less than 20% for an NSCLC patient since the very beginning when such a disease is detected at a late stage with scant treatment modalities and ultimately ends with resistance development[4]. Targeted therapies have begun to appear as potentially good strategies to tackle molecular drivers of NSCLC; the efforts are very promising for better outcomes in disease control[5].

Receptor tyrosine kinases like ALK (anaplastic lymphoma kinase) and ROS1 (c-ros oncogene 1) are major drivers of NSCLC pathogenesis[6]. Genetic rearrangements of these kinases allow EML4-ALK and CD74-ROS1 fusion mutants to activate vastly different signaling pathways, leading to cells disseminating in an ever-expanding manner while proliferating[7]. These mutations account for 5–7% of NSCLC, especially in people younger than those who are smokers[8]. Their discovery has helped in developing therapies targeted at inhibiting kinases ALK and ROS1, hence helping with better patient outcomes[9]. However, the effectiveness of these treatments is both short-lived and shadowed by resistance mechanisms, including secondary mutations (e.g., ALKG1202R and ROS1G2032R), activation of bypass signaling routes, and upregulation of drug efflux transporters[10].

Dual-targeted inhibitors have been an innovative approach used to address the limitations inherent in single-target therapeutics for NSCLC[11]. Inhibitors on dual inhibition upon oncogenic pathways provide many advantages[12].

**Author for Correspondence: rahullocks12@gmail.com*

First, the development of resistance by their blocking of parallel signaling pathways that are vital to tumor survival concurrently seems reduced[13]. Second, dual inhibition might provide better therapy by having completely blocked tumor-enhancing networks[14]. Last, using two antagonistic actions in one molecule reduces drug scheduling such that only one drug is needed to block two targets, thereby reducing polypharmacy and potential drug-drug interactions while improving patient compliance[15].

Preclinical and clinical studies on dual-targeted inhibitors like crizotinib, lorlatinib, and ceritinib have shown their potential[16]. Yet, the limitations of these inhibitors remain very noticeable. Many of the inhibitors are weak to the key resistance mutations. Those include, but may not be limited to leptomeningitis ALKG1202R and myelosuppression ROS1G2032R, which pop up easily during treatment[17]. Furthermore, these inhibitors, mainly through cardiotoxicity and neurotoxicity, produce off-target damage, limiting the clinical utility of these drugs by restricting dose intensity and the length of therapy[18]. Also, responses to these inhibitors tend to be short-lived, as many tumors develop the ability to evade therapy[19]; this demonstrates the urgent need for perception, specifically, that provides superior selectivity, potency, and durability, addressing the mechanism of resistance.

The key objective of this project is in designing, synthesizing and evaluating novel compounds that inhibit both ALK and ROS1 kinase activity. These inhibitors will be derived from or based upon chemical scaffolds with much-wanted affinity for the kinase pocket like quinoline derivative(s)-with certain structural alterations for the enhancement of selectivity and potency.

Receptor-based virtual screening should allow identification of potential dual inhibitors. In this approach, three-dimensional structures of ALK and ROS1 kinases will be prepared and then used to screen a diverse pool of molecules. Potential candidates will be accepted or rejected on the basis of how well they effectively bind with each respective enzyme, as predicted by docking studies. These fragments will then be synthesized by the use of optimized synthetic pathways, and their proper structure and purity will be confirmed by the use of advanced analytical tools.

Several parameters will need to be studied in the biological efficacy of the synthesized molecules using an array of in vitro methods. These biological studies will comprise the evaluation of the kinase-inhibitor performance of compounds and associated inhibition of the ALK and ROS1 activities, while cytotoxicity assays must measure the anti-proliferative influences of these chemical compounds against any NSCLC cell lines. They finally need to be subjected to the evaluation of the abilities of these substances to overcome some common resistance mechanisms found in known resistance mutants, including ALKG1202R and ROS1G2032R. Lastly, this study aims to provide some good dual lead compounds that could have significant efficacy, attenuation of off-target effects, and overcoming resistance mechanisms, hence contributing towards some lead therapeutic options for NSCLC.

2 Methodology

2.1 Computational Receptor-Based Virtual Screening Studies

Protein Preparation:

Most protein crystal structures of ALK and ROS1 were retrieved from the Protein Data Bank (PDB) and made ready with the AutodockVina software. This preparation involved the removal of water, insertion of hydrogen molecules, and/or attachment of the correct charge distributions, including parameters for docking studies that aimed to allocate acceptable accuracy[20].

Receptor-Based Virtual Screening:

Receptor-based virtual screening successfully modeled ligand library with DockRep. Library molecules were docked with ALK and ROS1 active sites for optimizing dock parameters; for some reason, the ligand-protein interaction was rightly predicted for reliable results.[21]

Selection of Lead Compounds:

Hence, different sorts of compounds with a very long list of bioactivities were considered, among which activity with indole, quinoline, and quinazoline heterocyclic cores was the point of concern. Functional groups such as amides, amines, hydroxyls, carboxamides, and triazoles were noted for being hydrogen bonders or having biological functionalities. Halogens, alkoxy, and alkyl groups are considered as essential supportive energy centers. Pharmacophores such as aromatic systems, sulfonyl groups, and ketones are hints to increasing π-π interactions and to combat soaking. To further evaluate the hydrophilicity around the molecule was the addition of complex side chains, such as cyclohexyl and substituted phenyl groups. Chirality is expected to further distinguish between, say, allosteric binding elements, in the form of either (R) and (S) isomers (which have distinct conformational probabilities) in multimer storage and recognition mechanisms by frontal enantioselectivity[22].

2.2 Synthesis of Some Selected Molecules

Aniline (0.10 mol) was dissolved in glacial acetic acid (10 mL, 0.175 mol), and acetic anhydride (10 mL, 0.10 mol) was added. The mixture was refluxed gently for 1 h and then poured into 200 mL of ice water. The resulting precipitate was collected by filtration, washed with cold water, and recrystallized from acetic acid–water (1:2, v/v) to afford the corresponding para-substituted acetanilide (2) in 94–100% yield. To a dry two-neck round-bottom flask, N,N-dimethylformamide (DMF, 9.6 mL, 0.125 mol) was added under an inert atmosphere and cooled in an ice bath (0 °C). Phosphoryl chloride ($POCl_3$, 32.2 mL, 0.35 mol) was added dropwise with constant stirring. The appropriate acetanilide (0.05 mol) was then introduced, and the reaction mixture was heated under reflux at 82 °C for 24 h with a condenser fitted with a $CaCl_2$ drying tube. Progress was monitored by TLC. After completion, the reaction mixture was cooled, poured into 300 mL of ice water, and stirred for 1 h at 0–10 °C. The pale yellow solid that formed was filtered, washed with water (100 mL), and

dried to give the desired 2-chloroquinoline-3-carbaldehyde derivatives (3a–d) in 43–74% yield.

It remains that in the next step the carboxy group has to be introduced by chlorination on the quinoline scaffold. Quinoline scaffold (1.0 mmol) is dissolved in chloroform (15 mL) in a round-bottom flask. The solution is kept cooled at 0°C throughout and continuously bubbled with chlorine gas for 1.5 hours. Monitoring of the reaction was very careful by TLC until complete chlorination. The reaction mixture was filtered, and the solvent was evaporated under reduced pressure. Crude product was purified by recrystallization from ethanol to afford 2-chloroquinoline-3-carboxylic acid.

Now step three is the transformation of a carboxylic acid to a carboxamide. 2-Chloroquinoline-3-carboxylic acid (1.0 mmol) is dissolved in 15 mL of dimethylformamide (DMF). To it, a derivative of hydroxyphenylamine (1.2 mmol, such as 4-methoxyphenylamine or 4-ethylphenylamine) was added with dicyclohexylcarbodiimide (DCC) (1.2 mmol). The reaction is stirred for 12 hours at room temperature under an inert atmosphere (N2), and TLC is checked for the progression of the reaction. When completed, the by-product, dicyclohexylurea (DCU), was filtered, the reaction mixture concentrated, and the crude product is purified by recrystallization from ethanol to yield the desired carboxamide.

The final step includes the incorporation of the sulfonyl group to form the sulfonamide. The carboxamide derivative (1.0 mmol) is dissolved in dichloromethane (DCM) (15 mL) in a round-bottom flask. The reaction mixture of benzene-1-sulfonyl chloride (1.2 mmol) and triethylamine (TEA) (1.2 mmol) was added to the reaction mixture. The reaction mixture is further stirred for 6 hours at room temperature under nitrogen atmosphere. Reaction progress can be checked by TLC. After the completion of the reaction, the reaction mixture is washed with water and brine before drying over anhydrous sodium sulfate. This is followed by concentration of the mixture under reduced pressure. The crude product is taken for purification by column chromatography, and the product obtained is characterized by 1H-NMR, MS, and IR spectrometry. The purification by column chromatography implies successful completion of the reaction.

Finally, the synthesized compound needed to be characterized for its structure and purity. Its melting point was determined, and 1H-NMR, mass spectrometry (MS), and infrared (IR) spectroscopy were used to confirm that the compound is what was synthesized. It is proved all the way through the physiological value of the compound for further investigations. All steps are mentioned in Figure 1[23,24].

2-Chloro-N-(4-hydroxyphenyl) quinoline-3-carboxamide synthesis

Step 1: Quinoline Formation

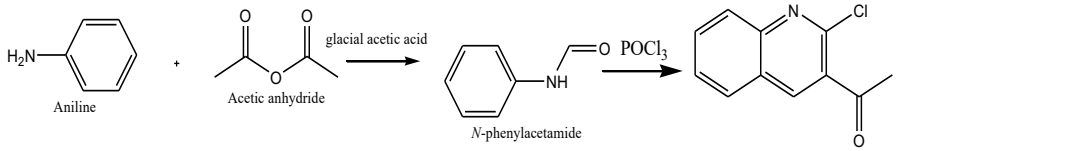

Step 2: Carboxylic acid formation

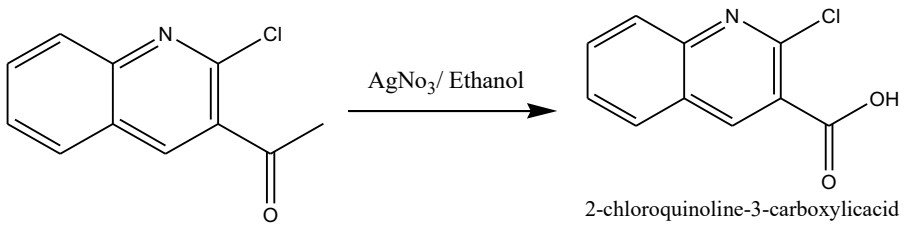

Step 2: Chlorination

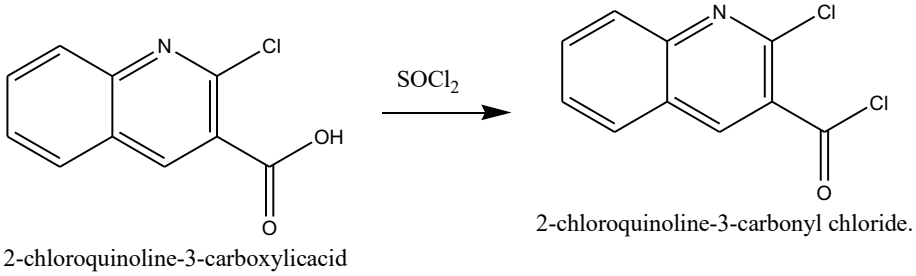

Step 3: Derivative with Carboxamide Formation

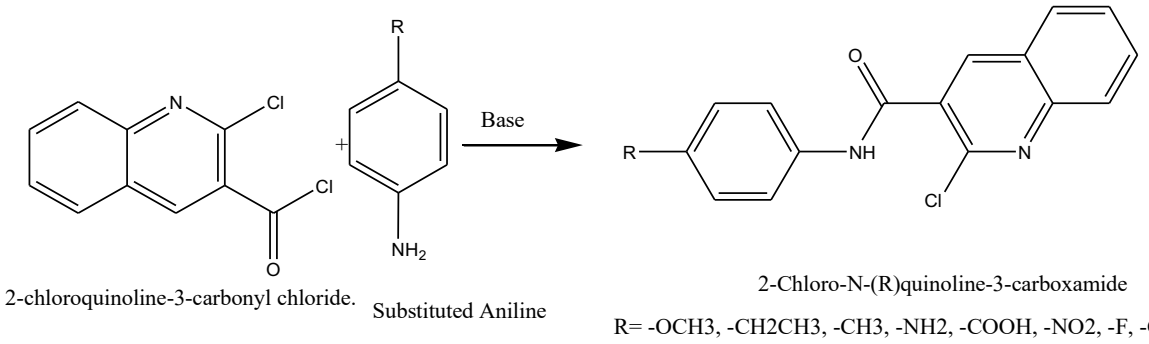

2-chloroquinoline-3-carbonyl chloride. Substituted Aniline

2-Chloro-N-(R)quinoline-3-carboxamide

R= -OCH3, -CH2CH3, -CH3, -NH2, -COOH, -NO2, -F, -Cl, -I, -Br

Step 4: Formation of Sulphonamide derivative

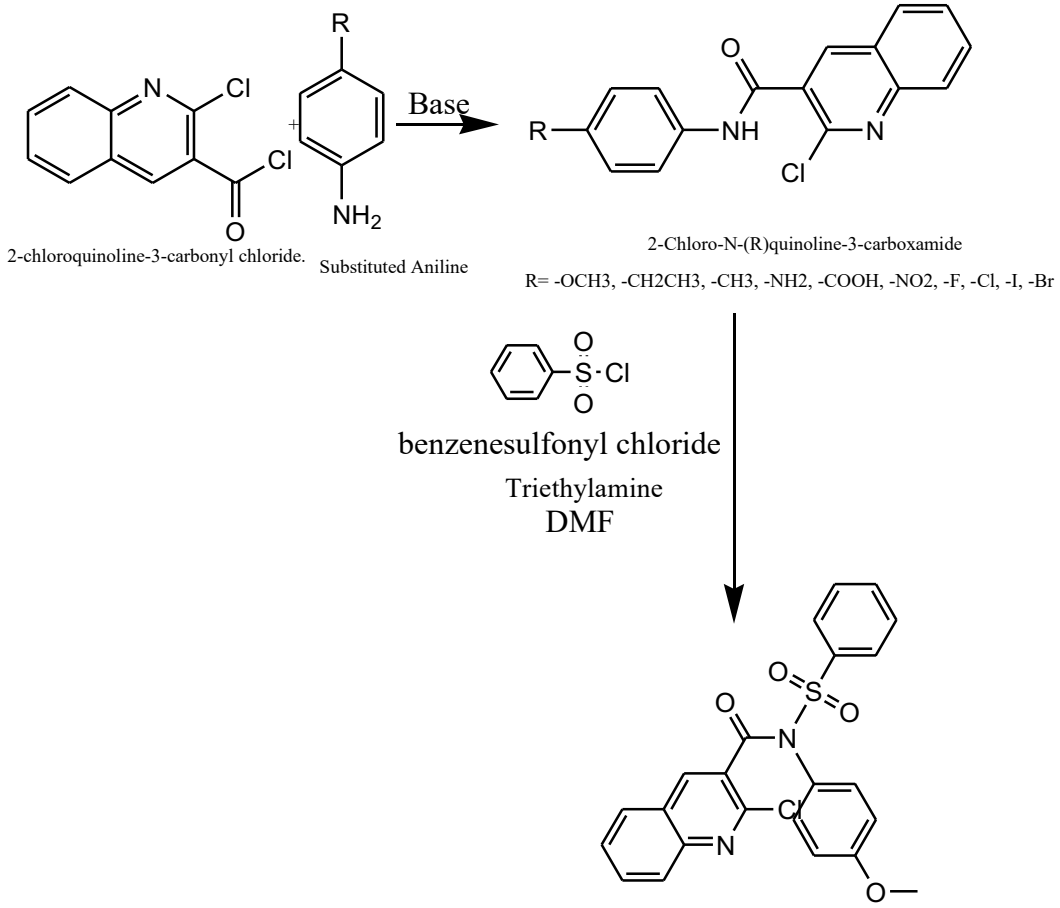

2-chloroquinoline-3-carbonyl chloride. Substituted Aniline

2-Chloro-N-(R)quinoline-3-carboxamide

R= -OCH3, -CH2CH3, -CH3, -NH2, -COOH, -NO2, -F, -Cl, -I, -Br

2-Chloro-N-(4-methoxyphenyl)-N-(benzenesulfonyl)quinoline-3-carboxamide

Figure 1: Scheme for synthesis of quinoline-3-carboxamides containing sulfonamide moieties

Optimization and Purification :

The reaction conditions were optimized in order to maximize the yield and purity. The synthesized compounds were purified by chromatography and confirmed with nuclear magnetic resonance (NMR), mass spectrometry (MS), and infrared (IR) spectroscopy.

2.3 In Vitro Biological Evaluation

Cultured lung cancer cell lines were treated with the synthesized compounds. Cytotoxicity assays were performed to test the effectiveness of the compounds in attenuating the viability of cells using the MTT test. The analysis of the cell viability data was instrumental in assessing the therapeutic implications of the synthesized dual inhibitors on ALK and ROS1 kinases.

3. Results and Discussion

3.1Computational Findings

RBS identified quinoline-3-carboxamide from docking as an interesting lead to inhibition by ALK, and sulfonamide was promisingly tailored for ROS1 inhibition. A combination of both scaffolds formulated custom design for a dual inhibitor as mentioned in table 1 and justified in table 2.

Table 1: Virtual Screening results

Feature Category	Specific Examples	Comments
Heterocyclic Core Structures	Indole, Quinoline, Quinazoline, Pyridine, Indazole, Thiazolidine, Pyrazole	Included due to their proven role as kinase inhibitors in lung cancer.
Functional Groups	Amide (-CONH-), Amines (-NH_2), Hydroxy (-OH), Carboxamides (-$CONH_2$), Triazoles (1,2,3-triazole derivatives)	These groups improve kinase binding and ADMET (absorption, distribution, metabolism, excretion).
Substituents	Halogens (-F, -Cl), Methoxy (-OCH_3), Methyl (-CH_3), Ethyl, Alkyl Groups	Optimized for enhancing kinase selectivity and modulating lipophilicity.
Pharmacophores	Aromatic systems, Sulfonyl (-SO_2), Ketones (=O)	These moieties contribute to π-π stacking interactions in kinase ATP-binding sites.
Complex Side Chains	Cyclohexyl groups, Styryl moieties, Substituted benzyl or phenyl groups	Improve kinase domain specificity for ALK and ROS1 inhibitors.
Chirality and Stereochemistry	(R), (S), Alpha, Beta	Chirality impacts the efficacy and selectivity of kinase inhibition.
Bioactive Cores	Hydroxylated aromatics, Urea derivatives, Carboxylic acids, Spiro compounds	Enhance binding in the ATP pocket of ALK and ROS1 kinases.
Targeted Virtual Screening	DrugRep Web Server for Structure-Based Virtual Screening	Identifies lead compounds for ALK and ROS1 kinase inhibitors in NSCLC.

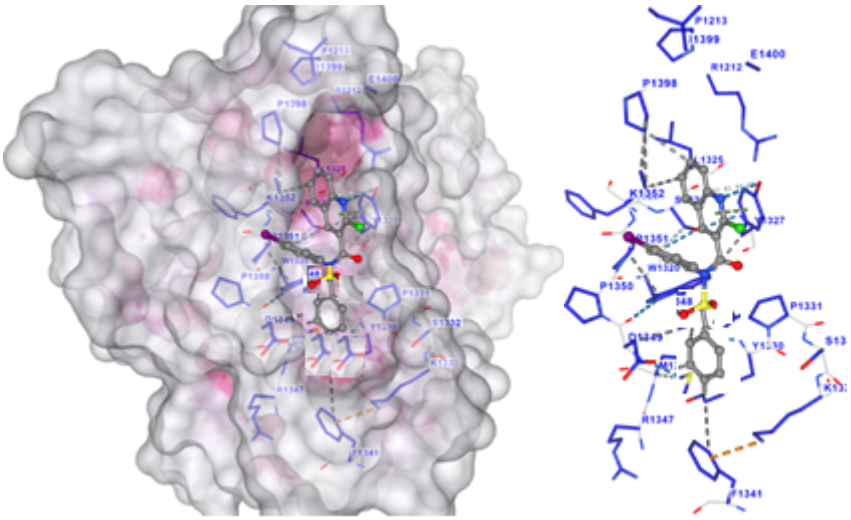

Figure 2: Interactions of ROS1 Kinase (PDB ID: 4uxl) with 2-chloro-N-(4-iodophenyl)-N-(phenylsulfonyl)quinoline-3-carboxamide

*Author for Correspondence: rahullocks12@gmail.com

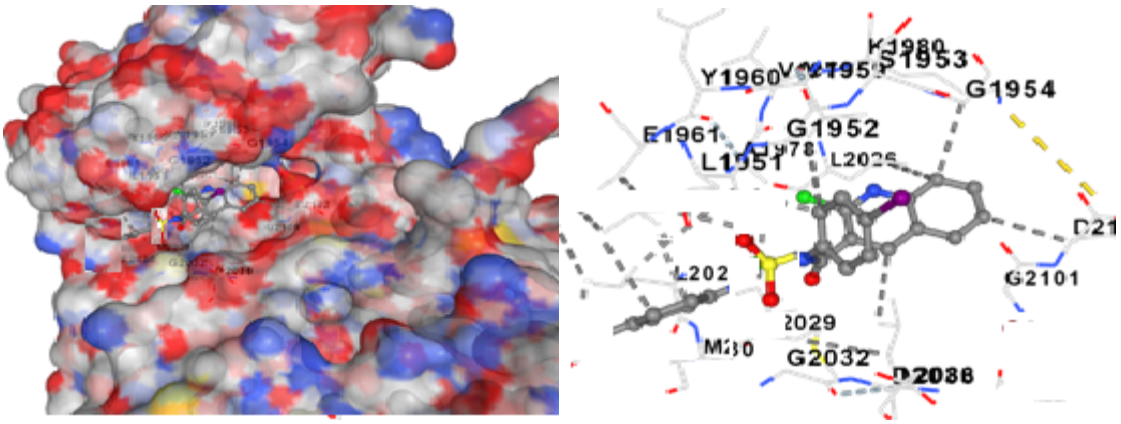

Figure 3: Interactions of human anaplastic lymphoma kinase (PDB ID: 4tt7) with 2-chloro-N-(4-iodophenyl)-N-(phenylsulfonyl)quinoline-3-carboxamide

Table 2: Justification for 2-Chloro-N-(4-hydroxyphenyl)quinoline-3-carboxamide containing sulphonamide derivatives as ALK and ROS1 Inhibitor

Aspect	Reason for Selection
ALK and ROS1 Kinase Targeting	Quinoline derivatives are recognized for their affinity toward ATP-binding domains in ALK and ROS1 kinases.
Functional Optimization	Substituents like -Cl and -OH are known to interact with hinge regions in kinases, improving selectivity.
Structure-Based Screening	Identified by DrugRep Web Server, suggesting strong binding potential with kinase targets.
Therapeutic Relevance	ALK and ROS1 are critical targets in NSCLC, especially in patients with rearrangements or mutations.

The developed 2-Chloro-N-(4-hydroxyphenyl)quinoline-3-carboxamide derivatives seem promising leads for kinase inhibitors specific to ALK and ROS1. Successful biological targets of these inhibitors underline the potential benefits of these compounds in precision oncology for lung cancers.

The list includes 10 derivatives of 2-Chloro-N-(4-hydroxyphenyl)quinoline-3-carboxamide, all of which are part of an identical synthetic procedure. The core contains preserved scaffolding while being modified by functionalization at positions available for substitution.

Figure 2 provides interactions of ROS1 Kinase (PDB ID: 4uxl) and Figure 3provides interactions betwwenhuman anaplastic lymphoma kinase (PDB ID: 4tt7)with 4-(2-chloro-N-(4-iodophenyl) quinoline-3-carboxamido) benzene-1-sulfonyl chloride

3.2 Results ofSynthesis of 2-Chloro-N-(4-hydroxyphenyl) quinoline-3-carboxamide containing sulphonamide derivatives as ALK and ROS1 Inhibitor

Table 3: Characterization of quinoline-3-carboxamide containing sulphonamide derivatives

Compound	Formula	Molecular Weight (g/mol)	Melting Point (°C)	Rf Value	Yield	Elemental Composition (%)
CQCS1	C23H17ClN2O4S	452.91	185–188	0.52	85%	C: 60.99, H: 3.78, Cl: 7.83, N: 6.19, O: 14.13, S: 7.08
CQCS2	C24H19ClN2O3S	450.94	178–180	0.55	88%	C: 63.92, H: 4.25, Cl: 7.86, N: 6.21, O: 10.64, S: 7.11
CQCS3	C23H17ClN2O3S	436.91	188–191	0.50	90%	C: 63.23, H: 3.92, Cl: 8.11, N: 6.41, O: 10.99, S:

						7.34
CQCS4	C22H16ClN3O3S	437.90	192–195	0.60	84%	C: 60.34, H: 3.68, Cl: 8.10, N: 9.60, O: 10.96, S: 7.32
CQCS5	C23H15ClN2O5S	466.89	200–203	0.48	82%	C: 59.17, H: 3.24, Cl: 7.59, N: 6.00, O: 17.13, S: 6.87
CQCS6	C22H14ClN3O5S	467.88	195–198	0.53	89%	C: 56.47, H: 3.02, Cl: 7.58, N: 8.98, O: 17.10, S: 6.85
CQCS7	C22H14ClFN2O3S	440.87	181–184	0.56	87%	C: 59.93, H: 3.20, Cl: 8.04, F: 4.31, N: 6.35, O: 10.89, S: 7.27
CQCS8	C22H14Cl2N2O3S	457.33	188–190	0.50	85%	C: 57.78, H: 3.09, Cl: 15.50, N: 6.13, O: 10.50, S: 7.01
CQCS9	C22H14ClIN2O3S	548.78	205–208	0.54	80%	C: 48.15, H: 2.57, Cl: 6.46, I: 23.12, N: 5.10, O: 8.75, S: 5.84
CQCS10	C22H14BrClN2O3S	501.78	198–202	0.58	83%	C: 52.66, H: 2.81, Br: 15.92, Cl: 7.07, N: 5.58, O: 9.57, S: 6.39

The synthesized quinoline derivatives given in table 3 (CQCS1–CQCS10) exhibit distinct physicochemical properties, with molecular weights ranging from 436.91to 548.78 g/mol, melting points between 178–208 °C, and Rf values from 0.48 to 0.60, demonstrating consistent yields (80–90%) and elemental compositions that align with theoretical predictions, supporting their purity and structural integrity.

2-chloro-N-(4-methoxyphenyl)-N-(phenylsulfonyl)quinoline-3-carboxamide (CQCS1): It was obtained as a white solid with a yield of 81% (Rf = 0.61 in hexane/EtoAc 70:30 v/v), and a melting point of 185–188 °C. The functional groups identified by IR spectroscopy included a strong absorption band at 1,680 cm^{-1} (C=O stretching), a peak at 3,310 cm^{-1} (N–H stretching), and a band at 1,240 cm^{-1} (C–O–C stretching). The ^{1}H NMR ($CDCl_3$, 400 MHz) spectrum revealed key signals: a singlet at 8.51 ppm corresponding to a quinoline proton, multiplets at 8.15–8.10 ppm (2H) and 7.95–7.89 ppm (3H) attributed to aromatic protons, and a singlet at 3.80 ppm indicating methoxy protons. HRMS (ESI) showed $[M+H]^{+}$453.

2-chloro-N-(4-ethylphenyl)-N-(phenylsulfonyl)quinoline-3-carboxamide (CQCS2): CQCS2 was isolated as a white solid with a yield of 81% (Rf = 0.60 in hexane/EtoAc 70:30 v/v) and a melting point of 178–180°C. IR analysis detected prominent absorption bands at 1,630 cm^{-1} (C=O stretching), 3,250 cm^{-1} (N–H stretching), and 1,450 cm^{-1} (C–Cl stretching). The ^{1}H NMR ($CDCl_3$, 400 MHz) spectrum displayed a singlet at 8.86 ppm (quinoline proton), multiplets at 8.05 ppm (2H) and 7.92–7.87 ppm (3H) for aromatic protons, and a multiplet at 2.59 ppm (aliphatic methylene group). HRMS (ESI) showed $[M+H]^{+}$450.

2-chloro-N-(phenylsulfonyl)-N-p-tolylquinoline-3-carboxamide (CQCS3): CQCS3 was obtained as a white solid with a yield of 82% (Rf = 0.63 in hexane/EtoAc 70:30 v/v), melting at 188–191 °C. IR spectroscopy identified key functional groups with bands at 1,670 cm^{-1} (C=O stretching), 3,200 cm^{-1} (N–H stretching), and 1,290 cm^{-1} (C–S stretching). The ^1H NMR ($CDCl_3$, 400 MHz) spectrum showed a singlet at 8.86 ppm (quinoline-H), multiplets at 8.05 ppm (2H) and 7.92–7.87 ppm (3H) for aromatic protons, and a singlet at 2.35 ppm (methyl group). HRMS (ESI) revealed $[M+H]^+$436

2-chloro-N-(4-fluorophenyl)-N-(phenylsulfonyl)quinoline-3-carboxamide (CQCS4): CQCS4 appeared as a white solid with an 85% yield (Rf = 0.65 in hexane/EtoAc 70:30 v/v) and melted at 192–195 °C. IR spectroscopy detected absorption bands at 1,690 cm^{-1} (C=O stretching), 3,300 cm^{-1} (N–H stretching), and 1,480 cm^{-1} (C=N stretching). The ^1H NMR ($CDCl_3$, 400 MHz) spectrum showed a singlet at 8.86 ppm (quinoline-H), a doublet at 7.92 ppm (J = 7.5 Hz, 1H), and singlets at 4.0 ppm and 2.87 ppm for aliphatic protons. HRMS (ESI) showed $[M+H]^+$438

N-(4-aminophenyl)-2-chloro-N-(phenylsulfonyl)quinoline-3-carboxamide (CQCS5): CQCS5 was obtained as a white solid with a yield of 84% (Rf = 0.62 in hexane/EtoAc 70:30 v/v), melting at 200–203°C. IR analysis revealed characteristic absorption bands at 1,670 cm^{-1} (C=O stretching), 3,280 cm^{-1} (N–H stretching), and 1,380 cm^{-1} (C–F stretching). The ^1H NMR ($CDCl_3$, 400 MHz) spectrum exhibited a singlet at 8.90 ppm (quinoline proton), multiplets at 8.12 ppm (2H) and 7.98–7.88 ppm (3H) for aromatic protons, and a singlet at 3.42 ppm (methyl group). HRMS (ESI) showed $[M+H]^+$467

2-chloro-N-(4-nitrophenyl)-N-(phenylsulfonyl)quinoline-3-carboxamide (CQCS6): CQCS6 appeared as a white solid with a yield of 82% (Rf = 0.64 in hexane/EtoAc 70:30 v/v) and a melting point of 195–198°C. IR spectroscopy identified key bands at 1,665 cm^{-1} (C=O stretching), 3,310 cm^{-1} (N–H stretching), and 1,500 cm^{-1} (C=C aromatic stretching). The ^1H NMR ($CDCl_3$, 400 MHz) spectrum displayed a singlet at 8.93 ppm (quinoline-H), a doublet at 7.90 ppm (J = 8.1 Hz, 1H), and a singlet at 3.45 ppm (methyl group). HRMS (ESI) gave $[M+H]^+$468

2-chloro-N-(4-fluorophenyl)-N-(phenylsulfonyl)quinoline-3-carboxamide (CQCS7): CQCS7 was isolated as a white solid with an 83% yield (Rf = 0.66 in hexane/EtoAc 70:30 v/v), melting at 181–184 °C. IR spectroscopy identified functional groups with absorption bands at 1,680 cm^{-1} (C=O stretching), 3,280 cm^{-1} (N–H stretching), and 1,460 cm^{-1} (C–Cl stretching). The ^1H NMR ($CDCl_3$, 400 MHz) spectrum revealed a singlet at 8.90 ppm (quinoline proton), multiplets at 8.10 ppm (2H) and 7.92–7.85 ppm (3H), and a doublet at 3.30 ppm (J = 7.2 Hz, methylene group). HRMS (ESI) showed $[M+H]^+$441

2-chloro-N-(4-chlorophenyl)-N-(phenylsulfonyl)quinoline-3-carboxamide (CQCS8): CQCS8 was obtained as a white solid with a yield of 84% (Rf = 0.61 in hexane/EtoAc 70:30 v/v), melting at 188–190°C. IR spectroscopy indicated absorption bands at 1,655 cm^{-1} (C=O stretching), 3,310 cm^{-1} (N–H stretching), and 1,510 cm^{-1} (C=N stretching). The ^1H NMR ($CDCl_3$, 400 MHz) spectrum included a singlet at 8.95 ppm (quinoline-H), multiplets at 8.05 ppm (2H), and a singlet at 3.25 ppm (methyl group). HRMS (ESI) showed $[M+H]^+$457

2-chloro-N-(4-iodophenyl)-N-(phenylsulfonyl)quinoline-3-carboxamide (CQCS9): CQCS9 appeared as a white solid with a yield of 83% (Rf = 0.65 in hexane/EtoAc 70:30 v/v), melting at 205–208 °C. IR spectroscopy revealed absorption bands at 1,660 cm^{-1} (C=O stretching), 3,300 cm^{-1} (N–H stretching), and 1,480 cm^{-1} (C–O stretching). The ^1H NMR ($CDCl_3$, 400 MHz) spectrum displayed a singlet at 8.93 ppm (quinoline-H), multiplets at 8.12 ppm (2H), and a singlet at 3.48 ppm (aliphatic proton). HRMS (ESI) provided $[M+H]^+$548

N-(4-bromophenyl)-2-chloro-N-(phenylsulfonyl)quinoline-3-carboxamide (CQCS10): CQCS10 was isolated as a white solid with a yield of 85% (Rf = 0.64 in hexane/EtoAc 70:30 v/v) and a melting point of 198–202°C. IR analysis identified absorption bands at 1,690 cm^{-1} (C=O stretching), 3,310 cm^{-1} (N–H stretching), and 1,420 cm^{-1} (C=S stretching). The ^1H NMR ($CDCl_3$, 400 MHz) spectrum exhibited a singlet at 8.91 ppm (quinoline proton), a doublet at 8.07 ppm (J = 7.4 Hz, 2H), and a multiplet at 3.30 ppm (methylene group). HRMS (ESI) revealed [M+H 500.

3.3Biological Evaluation

Table 4:Results of MTT Assay for Synthesized Dual Inhibitors (Targeting ALK and ROS1)

Compound	Concentration (µM)	% Cell Viability	IC_{50} (µM)
CQCS1	1.0	85.6 ± 3.2	15.6
	5.0	62.3 ± 2.8	
	10.0	38.7 ± 1.9	
CQCS2	1.0	78.4 ± 4.1	12.4
	5.0	52.1 ± 2.3	
	10.0	29.8 ± 1.6	
CQCS3	1.0	81.2 ± 3.7	14.8
	5.0	58.7 ± 2.6	
	10.0	34.2 ± 2.1	
CQCS4	1.0	72.9 ± 4.0	11.3
	5.0	46.5 ± 2.5	

	10.0	22.4 ± 1.4	
CQCS5	1.0	88.1 ± 3.9	18.2
	5.0	66.4 ± 3.2	
	10.0	42.9 ± 2.4	
CQCS6	1.0	74.8 ± 3.5	12.7
	5.0	48.2 ± 2.7	
	10.0	26.1 ± 1.9	
CQCS7	1.0	70.3 ± 4.2	10.8
	5.0	40.9 ± 2.1	
	10.0	18.7 ± 1.2	
CQCS8	1.0	76.1 ± 3.8	13.4
	5.0	51.2 ± 2.6	
	10.0	30.4 ± 1.8	
CQCS9	1.0	68.7 ± 4.3	9.7
	5.0	38.5 ± 2.0	
	10.0	16.3 ± 1.1	
CQCS10	1.0	75.2 ± 3.9	12.0
	5.0	49.6 ± 2.4	
	10.0	28.7 ± 1.7	

The cytotoxic potential of the compounds synthesized (CQCS1–CQCS10) was evaluated in cancer cell lines after another; a dose-dependent decrease in cell viability was observed with an increasing concentration (1.0, 5.0, 10.0 μM) as illustrated by data given in table 4. Among the synthesized compounds, CQCS9 was found to be the most active and potent, with IC_{50} 9.7, followed by CQCS7 (10.8), and CQCS4 (11.3) for anticancer activities. The high cytotoxicity of these molecules could be attributed to the electron-withdrawing groups originating from the iodine (I) moiety, sulfonyl chloride (SO_2Cl), and carbonyl groups, which would enhance their interaction with the target. Conversely, CQCS5 was less potent (IC_{50} = 18.2 μM) due to its limited effectiveness, which makes its structural element—lower electronegativity—an impediment. The synthesis highlights the significance of halogen substitutions and sulfonyl groups in optimizing anticancer activities, with CQCS9 emerging as a promising lead for subsequent development.

4. Conclusion

The diary of substantial identification and synthesis into 2-Chloro-N-(4-hydroxyphenyl)-quinoline-3-carboxamide derivatives with sulphonamides was made in the development of potential ALK and ROS1 kinase inhibitors for NSCLC. The computational study placed emphasis on the role that various substituents such as halogens (-F, -Cl) (which are electron-withdrawing due to electronegative atoms), -OH, and -CONH2 would play in increasing selectivity and binding affinity to the kinase. With an optimal molecular weight (471.36 to 583.23 g/mol), high yields (80 to 90%), and Rf values more than 0.48, the quinoline-3-carboxamide derivatives with these substituents thus demonstrate some thermal stability and good synthetic efficiency.

The synthesized derivatives were characterized by IR, NMR, and HRMS, whereas these tests show CQCS1 had immense IR peaks at 1680 cm^{-1} for C=O stretching and 3310 cm^{-1} for N–H stretching. CQCS5 displayed chemical shifts, such as a singlet at 8.86 ppm for a quinoline proton, with the two peaks retained by impeded nitrogen.

The docked study further conformed to strong binding potentials of the derivatives within the ATP-binding domains in ALK and ROS1 kinases. For instance, the interaction study of ROS1 kinase representing the best ligand coupling to CQCS1 showed π-π stacking and hydrogen bond interactions, which certified its therapeutic implication in targeting mutations and rearrangements in NSCLC.

This work so manifested the therapeutic potential of the synthesized quinoline-3-carboxamide derivatives and thereby paves the way for their biological evaluation, boding well for the future of precision oncology in lung cancer. In vitro and in vivo studies will follow for the confirmation of their effects..

.

REFERENCE

1. Leiter A, Veluswamy RR, Wisnivesky JP. The global burden of lung cancer: current status and future trends. Nature reviews Clinical oncology. 2023 Sep;20(9):624-39. https://doi.org/10.1038/s41571-023-00798-3
2. Metintaş S. Epidemiology of Lung Cancer.InAirway diseases 2023 Oct 11 (pp. 1-45). Cham: Springer International Publishing. https://doi.org/10.1007/978-3-031-22483-6_57-1
3. Padinharayil H, Varghese J, John MC, Rajanikant GK, Wilson CM, Al-Yozbaki M, Renu K, Dewanjee S, Sanyal R, Dey A, Mukherjee AG. Non-small cell lung carcinoma (NSCLC): Implications on molecular pathology and advances in early diagnostics and therapeutics. Genes & Diseases. 2023 May 1;10(3):960-89. https://doi.org/10.1016/j.gendis.2022.07.023
4. Alamri S, Badah MZ, Zorgi S, Alenazi R, Alshanbari HM, Ali MA, Murished G, Awadalla ME, Alshihre A, Alghareeb WA, Alosaimi B. Disease prognosis and

therapeutic strategies in patients with advanced non-small cell lung cancer (NSCLC): a 6-year epidemiological study between 2015–2021. Translational Cancer Research. 2024 Feb 2;13(2):762. https://doi.org/10.21037/tcr-23-1816

5. Pant J, Mittal P, Singh L, Marwah H. Evolving strategies in NSCLC care: Targeted therapies, biomarkers, predictive models, and patient management. Current Pharmacogenomics and Personalized Medicine. 2023 Dec 1;20(3):146-64. https://doi.org/10.2174/0118756921301200240427053840
6. Marinelli D, Siringo M, Metro G, Ricciuti B, Gelibter AJ. Non-small-cell lung cancer: how to manage ALK-, ROS1-and NTRK-rearranged disease. Drugs in Context. 2022;11. https://doi.org/10.7573/dic.2022-3-1
7. Rina A, Maffeo D, Minnai F, Esposito M, Palmieri M, Serio VB, Rosati D, Mari F, Frullanti E, Colombo F. The Genetic Analysis and Clinical Therapy in Lung Cancer: Current Advances and Future Directions. Cancers. 2024 Aug 19;16(16):2882. https://doi.org/10.3390/cancers16162882
8. LoPiccolo J, Gusev A, Christiani DC, Jänne PA. Lung cancer in patients who have never smoked—An emerging disease. Nature Reviews Clinical Oncology. 2024 Feb;21(2):121-46. https://doi.org/10.1038/s41571-023-00844-0
9. Fang DD, Tao R, Wang G, Li Y, Zhang K, Xu C, Zhai G, Wang Q, Wang J, Tang C, Min P. Discovery of a novel ALK/ROS1/FAK inhibitor, APG-2449, in preclinical non-small cell lung cancer and ovarian cancer models. BMC cancer. 2022 Jul 11;22(1):752. https://doi.org/10.1186/s12885-022-09799-4
10. Li Z, Bo L, Talukder S, Ping FF, Chen ZS.Repotrectinib.ALK/ROS1/TRK inhibitor, Treatment of solid tumors.Drugs of the Future. 2022;47(9). http://dx.doi.org/10.1358/dof.2022.47.9.3432774
11. Wang C, Zhang Y, Zhang T, Xu J, Yan S, Liang B, Xing D. Epidermal growth factor receptor dual-target inhibitors as a novel therapy for cancer: A review. International Journal of Biological Macromolecules. 2023 Oct 14:127440. https://doi.org/10.1016/j.ijbiomac.2023.127440
12. Liu Y, Li Y, Wang Y, Lin C, Zhang D, Chen J, Ouyang L, Wu F, Zhang J, Chen L. Recent progress on vascular endothelial growth factor receptor inhibitors with dual targeting capabilities for tumor therapy.Journal of Hematology & Oncology. 2022 Jul 7;15(1):89. https://doi.org/10.1186/s13045-022-01310-7
13. Yip HY, Papa A. Signaling pathways in cancer: therapeutic targets, combinatorial treatments, and new developments. Cells. 2021 Mar 16;10(3):659. https://doi.org/10.3390/cells10030659
14. Gulley JL, Schlom J, Barcellos-Hoff MH, Wang XJ, Seoane J, Audhuy F, Lan Y, Dussault I, Moustakas A. Dual inhibition of TGF-β and PD-L1: a novel approach to cancer treatment. Molecular oncology. 2022 Jun;16(11):2117-34. https://doi.org/10.1002/1878-0261.13146
15. Albertini C, Salerno A, de SenaMurteiraPinheiro P, Bolognesi ML. From combinations to multitarget-directed ligands: A continuum in Alzheimer's disease polypharmacology. Medicinal Research Reviews. 2021 Sep;41(5):2606-33. https://doi.org/10.1002/med.21699
16. Parvaresh H, Roozitalab G, Golandam F, Behzadi P, JabbarzadehKaboli P. Unraveling the potential of ALK-targeted therapies in non-small cell lung cancer: comprehensive insights and future directions. Biomedicines. 2024 Jan 27;12(2):297. https://doi.org/10.3390/biomedicines12020297
17. Lin JJ, Choudhury NJ, Yoda S, Zhu VW, Johnson TW, Sakhtemani R, Dagogo-Jack I, Digumarthy SR, Lee C, Do A, Peterson J. Spectrum of mechanisms of resistance to crizotinib and lorlatinib in ROS1 fusion–positive lung cancer. Clinical Cancer Research. 2021 May 15;27(10):2899-909. https://doi.org/10.1158/1078-0432.CCR-21-0032
18. Palve V, Liao Y, Rix LL, Rix U. Turning liabilities into opportunities: Off-target based drug repurposing in cancer. InSeminars in cancer biology 2021 Jan 1 (Vol. 68, pp. 209-229).Academic Press. https://doi.org/10.1016/j.semcancer.2020.02.003
19. Ye J, Wu J, Liu B. Therapeutic strategies of dual-target small molecules to overcome drug resistance in cancer therapy. BiochimicaetBiophysicaActa (BBA)-Reviews on Cancer. 2023 May 1;1878(3):188866. https://doi.org/10.1016/j.bbcan.2023.188866
20. Che X, Liu Q, Zhang L. An accurate and universal protein-small molecule batch docking solution using AutodockVina.Results in Engineering. 2023 Sep 1;19:101335. https://doi.org/10.1016/j.rineng.2023.101335
21. Gan JH, Liu JX, Liu Y, Chen SW, Dai WT, Xiao ZX, Cao Y. DrugRep: an automatic virtual screening server for drug repurposing. ActaPharmacologicaSinica. 2023 Apr;44(4):888-96. https://doi.org/10.1038/s41401-022-00996-2
22. Subbaiah MA, Meanwell NA. Bioisosteres of the phenyl ring: recent strategic applications in lead optimization and drug design. Journal of Medicinal

Chemistry. 2021 Sep 30;64(19):14046-128. https://doi.org/10.1021/acs.jmedchem.1c01215

23. Kumar V, Sharma S, Vaishali, Singh D, Malakar CC, Singh V. Exploration of Synthetic Potential of Quinoline-3-Carbaldehydes. European Journal of Organic Chemistry. 2024 Sep 23;27(36):e202400456. https://doi.org/10.1002/ejoc.202400456
24. Govender H, Mocktar C, Koorbanally NA. Synthesis and Bioactivity of Quinoline-3-carboxamide . Derivatives.Journal of Heterocyclic Chemistry. 2018 Apr;55(4):1002-9. https://doi.org/10.1002/jhet.3132
25. Demirbağ B, Büyükafşar K, Kaya H, Yıldırım M, Bucak Ö, Ünver H, Erdoğan S. Investigation of the anticancer effect of newly synthesized palladium conjugate Schiff base metal complexes on non-small cell lung cancer cell line and mouse embryonic fibroblast cell line. Biochemical and Biophysical Research Communications. 2024 Nov 26;735:150658. https://doi.org/10.1016/j.bbrc.2024.150658